



CO₂ Emissions in Layered Cranberry Soils under Simulated Warming

Wilfried Dossou-Yovo^{1,2,*}, Serge-Étienne Parent¹, Noura Ziadi² and Léon E. Parent^{1,*}

¹ Department of Soils and Agri-Food Engineering, Université Laval, Quebec, QC G1V 0A6, Canada

² Agriculture and Agri-Food Canada, Quebec Research and Development Center, 2560 Hochelaga Boulevard, Quebec, QC G1V 2J3, Canada

* Correspondence: wilfrieddossouyovo16@gmail.com (W.D.-Y.); leon-etienne.parent@fsaa.ulaval.ca (L.E.P.)

Abstract: Sanding to bury the overgrowth of uprights and promote new growth results in alternate sand and organic sublayers in the 0–30 cm layer of cranberry soils contributing to global carbon storage. The aim of this study was to measure CO₂ emission rates in cranberry soil sublayers under simulated warming. Soil samples (0–10, 10–20 and 20–30 cm) were incubated in jars for up to 105 days at 10, 20 and 30 °C. The CO₂ emission rate was measured biweekly by gas chromatography. The CO₂ emission rate increased with temperature and decreased in deeper soil sublayers. Linear regression relating CO₂ efflux to soil sublayer and temperature returned R² = 0.87. Sensitivity of organic matter decomposition to temperature was estimated as activation energy and as Q₁₀ coefficient, the increase in reaction rate per 10 °C. Activation energy was 50 kJ mol⁻¹, 59 kJ mol⁻¹ and 71 kJ mol⁻¹ in the 0–10, 10–20 and 20–30 cm sublayers, respectively, indicating higher molecular-weight compounds resisting to decomposition in deeper sublayers. The Q₁₀ values were significantly higher (*p* < 0.01) in the 10–30 cm (2.79 ± 0.10) than the 0–10 cm (2.18 ± 0.07) sublayers. The 20–30 cm sublayer where less total carbon was stored was the most sensitive to higher temperature. Cranberry soils could be used as sensitive markers of global warming.

Keywords: carbon accumulation; cranberry soils; activation energy; temperature-dependent CO₂ emissions rate



Citation: Dossou-Yovo, W.; Parent, S.-É.; Ziadi, N.; Parent, L.E. CO₂ Emissions in Layered Cranberry Soils under Simulated Warming. *Soil Syst.* **2023**, *7*, 3. <https://doi.org/10.3390/soilsystems7010003>

Academic Editor: Luis Eduardo Akiyoshi Sanches Suzuki

Received: 9 November 2022

Revised: 28 December 2022

Accepted: 30 December 2022

Published: 9 January 2023



Copyright: © 2023 by the authors. Licensee MDPI, Basel, Switzerland. This article is an open access article distributed under the terms and conditions of the Creative Commons Attribution (CC BY) license (<https://creativecommons.org/licenses/by/4.0/>).

1. Introduction

Terrestrial carbon (C) is three times greater than atmospheric C [1]. Soil C sequestration is the conversion of atmospheric CO₂ into long-lived C pools [2]. While soil C sink capacity of managed ecosystems is the estimated historic cumulative C loss of 55–78 Gt, the attainable capacity is only 50–66% of that potential [3]. Cranberry agroecosystems are exceptions to this general perspective [4]. The fate of organic matter in soils depends primarily on its intrinsic decomposability and on protection mechanisms such as soil aggregation [5] in silty or clayey agricultural soils [6].

In North America, conventionally and organically managed cranberry agroecosystems are mostly established on acid sandy soils arranged as flat beds in low-lying positions to facilitate water transfer [7]. Beds are diked, then capped with 0.3–1.0 m of sand. Native soil C is accumulated in dikes, beds, and the subsoil. The seasonal C flux of leaf and stem litterfall was estimated at 2.15–2.57 Mg C ha⁻¹ (153-d)⁻¹ in Wisconsin [8]. The belowground vegetative biomass may contribute up to 2/3 of total vegetative C stocks. The overgrowth of uprights is buried every 2–5 years by spreading two to five cm of sand onto frozen soil to promote new growth [9]. This results in alternate layers of sand and organic matter in the root zone [10] and high potential for C storage due to physical protection through anthropic surface sanding [4].

The composition and biomass of the microbial community generally differ between upper and lower soil layers [11–13]. The decreasing rates of CO₂ emissions in deeper soil layers [14,15] have been attributed to the vertical distribution of soil organic carbon in

terms of amount and quality [13–16]. Indeed, the C:N ratio is narrower, and soil organic matter (SOM) is more decomposed, in deeper layers of cranberry soils [10]. Temperature at depth should also be considered. The threshold temperature for mineralization activity of cranberry soil was set at 13 °C [8].

The effect of temperature on organic matter decomposition is crucial to understand the global C cycle and potential feedbacks to the climate system [17]. The largest C stocks have been found at high latitude [18,19]. While the seasonal CO₂ emission of Quebec cranberry soils has been estimated at 2.7–3.4 t CO₂ eq ha⁻¹ [20], the effect of global warming on CO₂ emission in the soil profile as a function of temperature has not been established. The activation energy of decomposition and the Q₁₀ coefficient as increase in reaction rate per 10 °C [17,21,22] can reflect the differential contribution of soil layers to CO₂ emissions in cranberry agroecosystems in areas of rapid climate change such as Eastern Canada.

We hypothesized that activation energy of soil organic matter (SOM) decomposition and Q₁₀ differ in alternate sand and organic matter layers due to the differential C/N ratio and decomposition degree of organic matter in two differently managed cranberry soils. The aim of this study was to measure the decomposition rate of SOM in layered cranberry soils as a function of management (conventional vs. organic), soil layer, incubation time and temperature under controlled environments to assess the differential effects of global warming on soil C storage in cranberry soils.

2. Materials and Methods

2.1. Soil Sampling and Analysis

Sites were selected to cover the two main management practices in south-central Quebec. Site #45 (46°16'34.7" N, 71°51'30.0" W, elevation 112 m) was conventionally managed, and site #A9 (46°14'16.5" N, 72°02'13.4" W, elevation 92 m) was organically farmed. Sites #45 and #A9 have been planted to cultivar "Stevens" in 1999 and 2004, respectively. The climate of the region is sub-humid temperate and continental with cold winters and hot summers. Soil series were the Saint-Jude series at site #45 and Sainte-Sophie series at site #9, both classified as Humo-Ferric Podzols in the Canadian System Haplorthods in the U.S. Soil Taxonomy, and Orthic Podzols in the World Reference Base for Soil Resources. The soil contained 937 g sand kg⁻¹, 37 g silt kg⁻¹, and 26 g clay kg⁻¹ at site #45, and 915 g sand kg⁻¹, 49 g silt kg⁻¹, and 36 g clay kg⁻¹ at site #9 [4].

Fields received 40 kg N ha⁻¹ yr⁻¹ as ammonium sulfate (site #45) or granules of poultry manure (site #9). The source of phosphorus was mono-ammonium phosphate at site #45 as recommended locally from soil and tissue tests, and granules of poultry manure at site #9 from a N-based recommendation. Potassium was applied at a rate of 100 kg K ha⁻¹ as KCl, sul-po-mag and/or granules of poultry manure. Micro-nutrients were applied at need depending on the results of tissue testing. Fields were sprinkler-irrigated at need.

Soil samples were collected for physical analyses in spring 2018. Three soil layers were sampled (0–10; 10–20; 20–30 cm) at four places per site using cylinders (diameter = 5.5 cm, height = 7.6 cm). Samples were sealed in plastic bags and stored at 4 °C until use within a week. Soil samples were air dried, and 2 mm sieved before analysis. Soil pH was measured in 0.01 M CaCl₂ (soil to solution ratio of 1:2 v:v). Soil carbon and nitrogen were quantified by combustion [23] using the Leco CNS model 630-300-200 (Leco Corporation, Saint-Joseph, MI, USA). Soil bulk density was determined as the mass of air-dry soil divided by the volume of the cylinder. Soil carbon content and porosity were computed in each 10 cm thick layers as follows [24]:

$$C_s = P_b \times C_c \quad (1)$$

$$C_{layer} = C_s \times [layer\ thickness] \times area \quad (2)$$

$$TP = (1 - P_b/P_p) \times 100 \quad (3)$$

$$P_d = \frac{100}{\frac{\%Organic\ matter}{1.55} + \frac{100 - \%Organic\ matter}{2.65}} \quad (4)$$

where C_s = carbon stock (kg m^{-3}), C_c = carbon content (%), TP is total soil porosity (volumetric fraction); P_b = soil bulk density (g cm^{-3}); P_d = soil particle density assuming 1.55 g cm^{-3} as the particle density of organic matter and 2.65 g cm^{-3} as the particle density of mineral matter [25].

2.2. CO_2 Emission

Soils were sampled at three depths (0–10 cm, 10–20 cm, 20–30 cm) and four locations in each field (785 mL per sample using cylinders 10 cm in height and 10 cm \varnothing) and introduced in plastic bags. The 72 fresh soil samples were 6 mm sieved, filled to 1/3 of the volume of 250-mL Mason jars with 100 g dry-based material, and placed in temperature-controlled chambers following a completely randomized design with four replications per site. There were three (3) soil layers (0–10; 10–20; 20–30 cm), three (3) temperatures (10, 20 and 30 °C), four (4) replicates and two (2) sites. Soil water content was adjusted twice a week with distilled water to water-filled pore space (WFPS) close to 0.50–0.70 as volumetric fraction [24,26]. Water content was assessed by weighing the jars, assuming a density of one g cm^{-3} .

Soil CO_2 flux was measured using a close chamber protocol [26]. At sampling time taken biweekly during 105 d, jars were capped with a lid containing two male slips. One slip was fitted to a septum for headspace sampling using a 20 mL polypropylene syringe. The other slip was used to equilibrate the jar internal pressure during sampling. Air samples were taken at 0 and 24 h, then transferred into pre-evacuated 12 mL glass vials (Exetainer, Labco, High Wycombe, UK). Gas samples were analyzed for CO_2 using a gas chromatograph fitted to a Ni- NO_3 (10%) catalyst column and a flame ionization detector (Model 3800, Varian Inc., Walnut Creek, CA, USA), equipped with a headspace auto-injector (Combi Pal, CTC Analytics, Zurich, Switzerland). The CO_2 flux (F_c , $\mu\text{g g}^{-1} \text{h}^{-1}$) was measured as [26].

$$F_c = \frac{dc}{dt} \times \frac{v}{M_v} \times \frac{M_m}{W}, \quad (5)$$

where dc/dt ($\mu\text{L L}^{-1} \text{h}^{-1}$) is change rate of headspace CO_2 concentration in dry air samples estimated at time = 0 and time = 24 h, assuming that CO_2 emissions vary linearly through time; v (L) is pot headspace volume; M_v (L mol^{-1}) is molecular volume at the pre-deployment air temperature (22–24 °C); M_m ($\mu\text{g mol}^{-1}$) is molecular mass of CO_2 (44,000,000); and W (g) is dry soil mass.

2.3. Statistical Analysis

2.3.1. First Order Kinetics

The decomposition rate constant (k) was computed as follows [27]:

$$k = \frac{\ln([C_{\text{initial}} - \text{CO}_2\text{-}C_t]/C_{\text{initial}})}{t} \quad (6)$$

where C_{initial} (mg kg^{-1}) is initial soil carbon content, and $\text{CO}_2\text{-}C_t$ (mg kg^{-1}) is cumulative CO_2 released during incubation period t .

2.3.2. Q_{10} and Activation Energy

The increase in reaction rate per 10 °C was reported as follows [21,22]:

$$Q_{10} = \frac{k \times (t + 10)}{k(t)} \quad (7)$$

where $k_{(t)}$ is k at temperature t (°K) and $k_{(t+10)}$ is k at temperature $t + 10$ (°K).

Activation energy was derived from the Arrhenius equation [19,22] as follows [21]:

$$k = A \times \exp(-E_a/RT) \quad (8)$$

where A is pre-exponential factor and Ea is activation energy assumed to be independent of temperature, R is the universal gas constant, and T is absolute temperature ($^{\circ}\text{K}$).

2.3.3. Statistical Analysis

Statistical analyses were performed in the R environment version 4.1.0 [28]. The difference between conventional and organic farming systems were tested using a mixed model. The CO_2 emission rates were fitted to elapsed time, temperature and soil layers across farming systems using the lm linear regression model as follows [29]:

$$y = \beta_0 + \beta_1 x_1 + \dots + \beta_k x_k + \varepsilon \quad (9)$$

where y (CO_2 emission rate) is the predicted value, x_1 through x_k are k independent variables or predictors (time, temperature in $^{\circ}\text{K}$, soil layers), β_0 is the value of y where independent variables take zero values, and β_1 through β_k are estimated regression coefficients. The R codes and dataset are available online at <https://bit.ly/3gbi6Ov> (accessed on 8 January 2023).

3. Results

3.1. Soil Properties

Soil properties are presented in Figure 1. Soil carbon content varied from 1.67 to $30.9 \text{ Mg C ha}^{-1}$, being larger in the 0–10 cm (16.55 ± 1.15), than in the 10–20 cm (13.63 ± 2.95) and the 20–30 cm (6.09 ± 1.44) layers (Figure 1A). The C:N ratios were 20.08 ± 1.05 , 16.01 ± 1.91 and 9.02 ± 1.96 in 0–10, 10–20 and 20–30 cm layers, respectively (Figure 1B). Soil bulk density increased in lower layers as a result of sand accumulation and organic matter decomposition while biomass production reduced bulk density in the upmost layer. Lower pH values in upper layers under conventional farming are attributable to soil acidification by elemental sulfur amendment and ammonium sulfate fertilization. In organic farming, high-ammonium poultry manure granules likely acidified the upper soil layer in the first place. Soil porosity, water content and bulk density followed the same trends as inter-related properties.

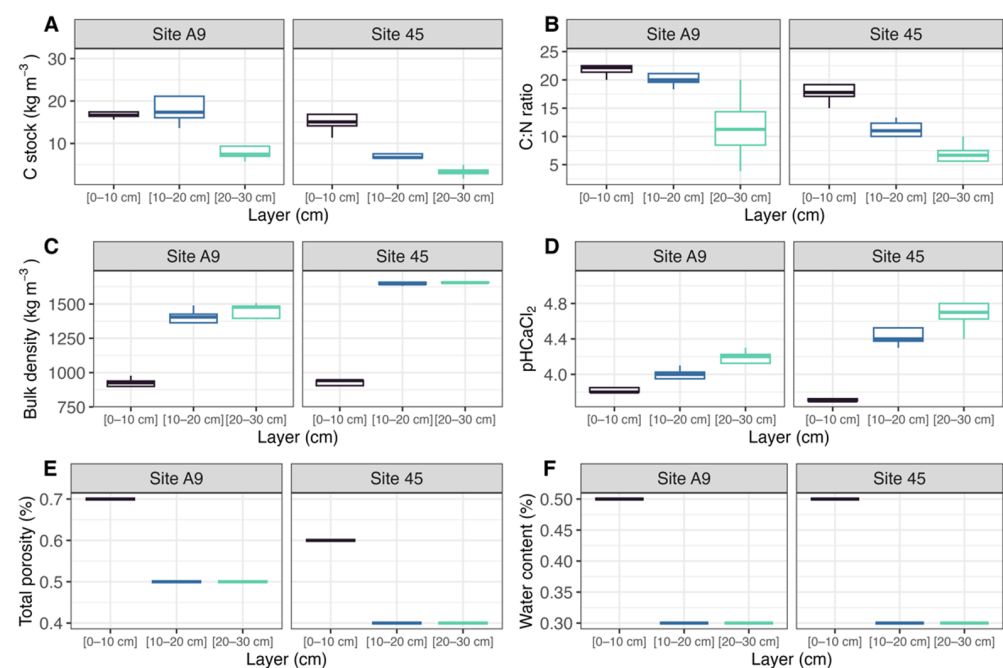


Figure 1. Soil properties in layers of cranberry soils: (A) C stock, (B) C:N ratio, (C) bulk density, (D) $\text{pH}_{\text{CaCl}_2}$, (E) total porosity (volumetric fraction), (F) water content (volumetric fraction).

3.2. CO₂ Emission Rate

The CO₂ emission rates did not differ significantly between sites (p -value > 0.05), decreased (p -value ≤ 0.05) through time and soil depth, and increased (p -value ≤ 0.05) with temperature (Figure 2). The soil layer showed the largest effect followed by temperature and incubation time. The CO₂ emissions are presented in Figure 3 for significant treatments.

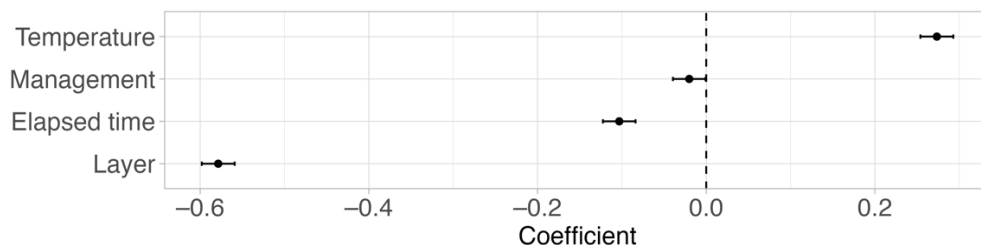


Figure 2. Effect of temperature, management, elapsed time and soil layer on CO₂ emissions. Probability for significance is 0.05.

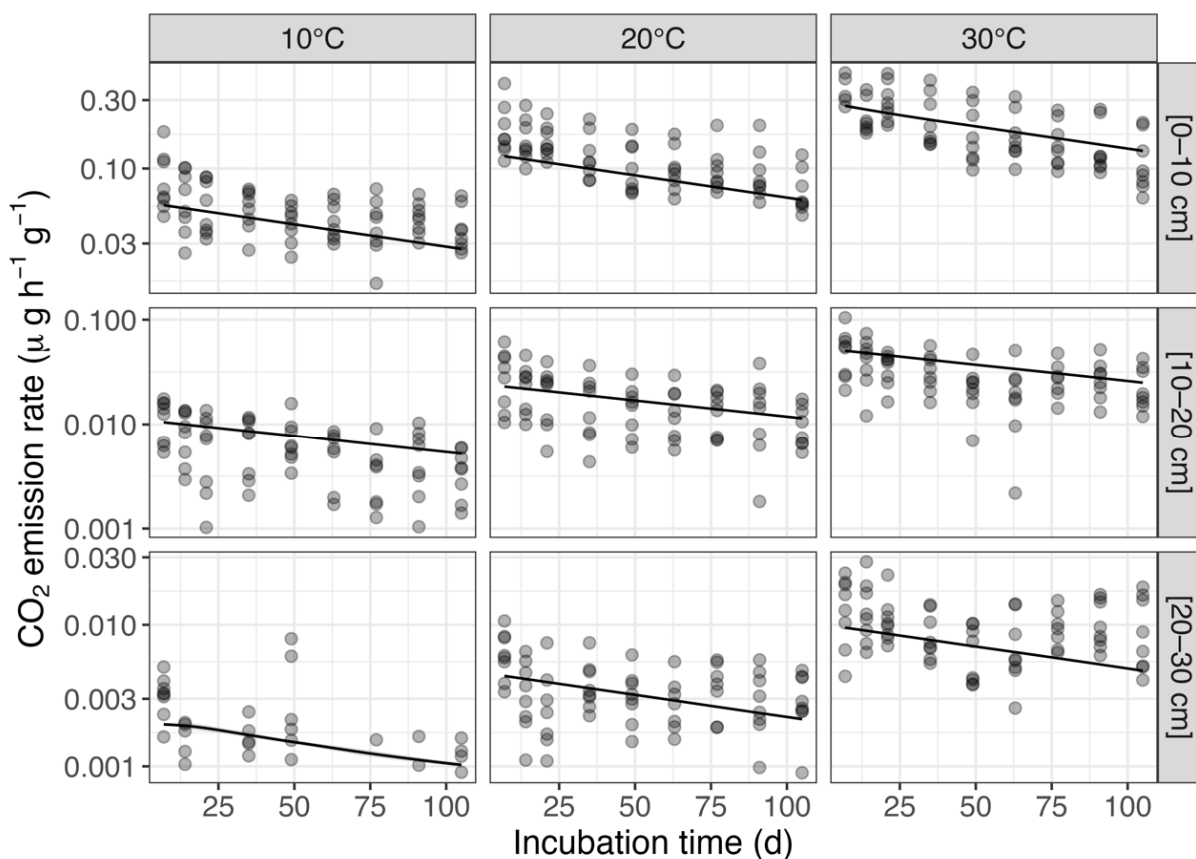


Figure 3. Influence of soil layer, temperature and time on CO₂ emission rate.

The CO₂ emission rate was highest in the 0–10 cm layer at 30 °C and lowest in the 20–30 cm layer at 10 °C. At 10 °C, 87.2% of the total across-layer CO₂ emissions during the incubation period occurred in the 0–10 cm layer compared to 12.1% in the 10–20 cm layer and 0.7% in the 20–30 cm layer. At 20 °C, 83.1% of total across-layer CO₂ emission occurred in the 0–10 cm layer compared to 14.3% in the 10–20 cm layer and 2.5% in the 20–30 cm layer. At 30 °C, 82.8% of total across-layer CO₂ emission occurred in the 0–10 cm layer compared to 13.5% in the 10–20 cm layer and 3.8% in the 20–30 cm layer. The R² value of the equation relating CO₂ emission to temperature, soil depth and elapsed time was 0.87 and root-mean-square-error was 0.24 (Figure 3).

The effect of temperature on SOM decomposition rates indicated large differences between layers in biochemical composition of the organic materials and SOM resistance to decomposition. The slope of the Arrhenius equation ($-Ea/R$) was highest in the (0–10 cm) layer, intermediate in the 10–20 cm layer and lowest in the 20–30 cm layer (p -value < 0.001) (Figure 4). The activation energy required to decompose SOM was 50 kJ mol⁻¹ in the 0–10 cm layer, 59 kJ mol⁻¹ in 10–20 cm layer and 71 kJ mol⁻¹ in 20–30 cm layer (Figure 5). The Q_{10} (mean \pm SE) was 2.79 ± 0.10 in the 20–30 cm layer and 2.18 ± 0.07 in the 0–10 and 10–20 cm layers (p -value < 0.001) (Figure 6).

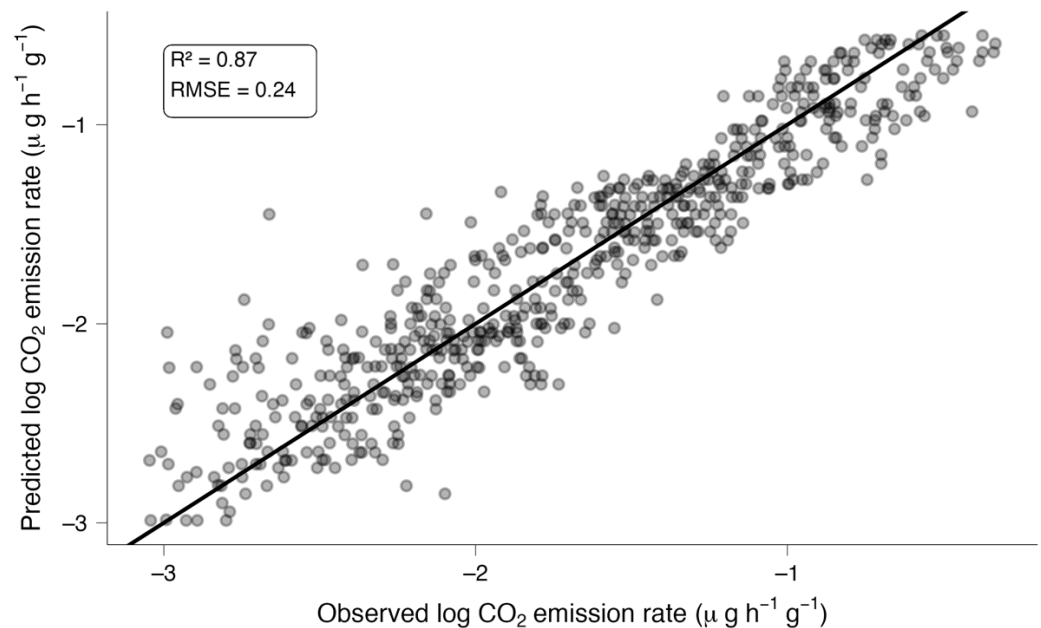


Figure 4. Relationship between observed and predicted CO₂ emission rates.

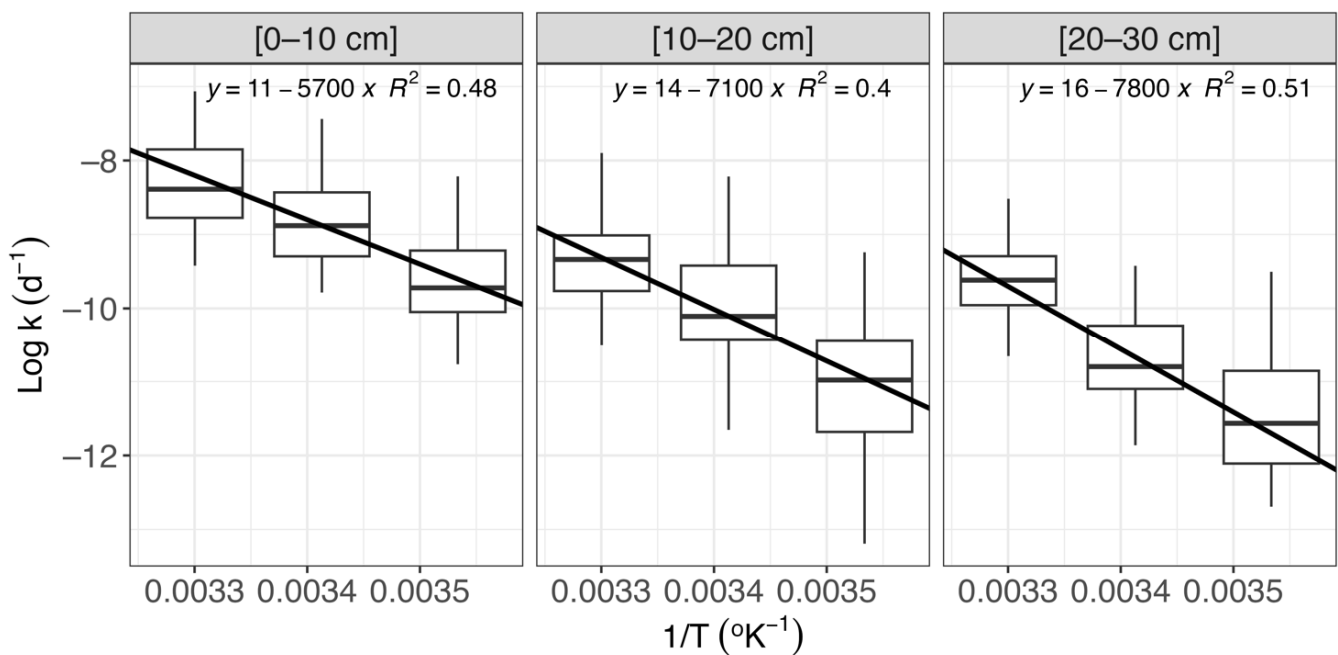


Figure 5. Experimental data fitted to the Arrhenius equation (p -value < 0.001).

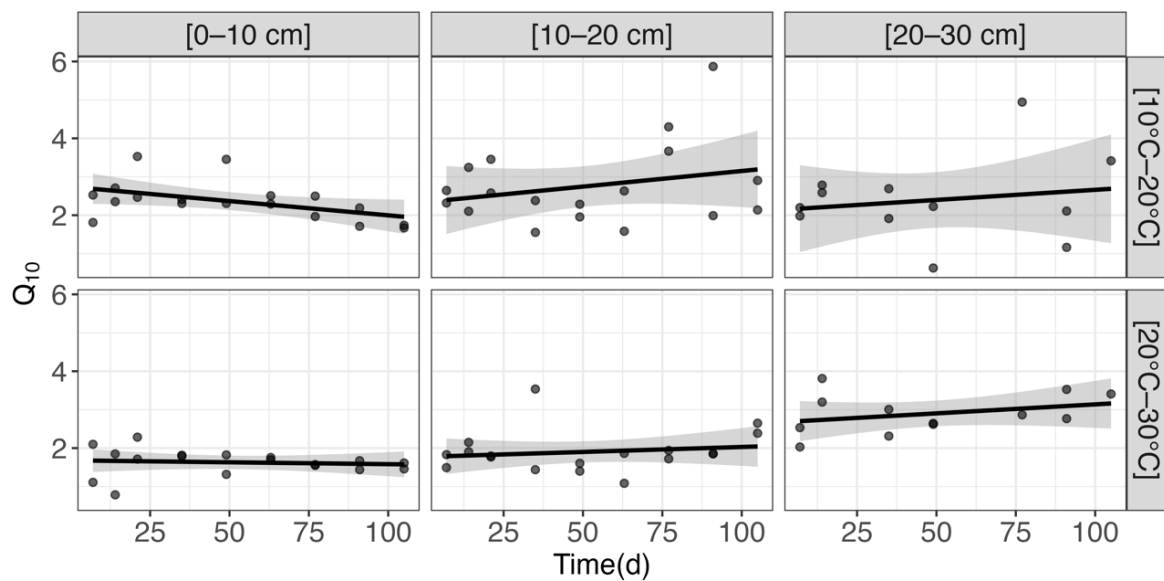


Figure 6. Time variation of Q_{10} across soil layers (p -value < 0.001).

4. Discussion

Several factors such as climate, the amount and quality of plant residues, soil management, mineralogy, texture [30–33], bulk density [34], as well as layer location in the soil profile [10,15,16,35,36] control organic matter turnover in soils. Organic matter decomposition rate also depends on the spatial distribution of organic matter, and the site-specific microbial community impacted by land use, temperature, rainfall, soil type and bulk density [12,37]. In cranberry soils documented in Figure 1, differences in soil parameters should be further addressed in relation with carbon accumulation and microbe abundance and diversity.

Cranberry agroecosystems were shown to contribute to CO_2 emissions much less ($2.7\text{--}3.4 \text{ t CO}_2 \text{ eq ha}^{-1}$) compared to other horticultural cropping systems [20]. Indeed, slowly decomposing carbon can accumulate in large amounts in layered cranberry soils after burial of organic matter through regular sanding. This paper quantified layer \times temperature interactions regulating CO_2 emissions in cranberry soils.

4.1. Dependency of CO_2 Emission on Soil Depth

The decreasing CO_2 emission rate in deeper soil layers results in part from the vertical distribution of soil organic carbon (SOC) in terms of amount and quality [16]. The biochemical composition varies considerably among cranberry soil layers [4]. The biochemical quality of plant species and that of the soil are the main factors driving litter decomposition under otherwise similar conditions of temperature and rainfall [38–40]. For example, litter quality differs considerably among tundra, grassland, and boreal, conifer, deciduous, and tropical forest biomes [38]. Litter decomposability is associated with species' ecological strategy within different ecosystems globally [39]. The effect of climate on litter mass loss can be offset by differences in soil parameters as mediated by soil microbial populations [40].

Fresh sources of SOC such as shoot litter, senescent roots, and root exudates [41,42] are directly available to soil microbes in upper layers [43]. Fresh organic matter decreases deeper in the soil profile [36,44,45]. There is abundant young fast-cycling C in upper layers compared to ancient slow-cycling C in the subsoil [36]. As a result, soil respiration is greater near soil surface (0–5 and 5–10 cm layers) compared to lower layers [46]. The cranberry litter deposited on the floor of cranberry beds contains approximately 80% of lignocellulose while 89% of the particles are larger than 2 mm in size and the C:N ratio is 55 in average [4]. Lignocellulose is a compact material made of strongly bound cellulose, lignin, and hemicellulose in structural networks in stems and roots [47]. Lignocellulose is

broken down by a suite of extracellular enzymes [48]. Due to structural and biochemical constraints, litter is slowly decomposed in cranberry soils [4].

4.2. Temperature Sensitivity on CO₂ Emission Rates

The activation energy required to decompose SOM in cranberry agroecosystems was lower in upper layers (50–59 kJ mol⁻¹) than in the 20–30 cm layer (71 kJ mol⁻¹) where high-molecular-weight phenolic compounds abound [4]. In comparison, the *E_a* values for enzyme activities were 75 kJ mol⁻¹ for phenol oxidase and, 40–45 kJ mol⁻¹ for β-glucosidase, cellobiohydrolase and peroxidase in the A horizons of three temperate biomes [48], compared to that of pyrophosphatase that averaged 22–33 kJ mol⁻¹ in Histosols and 33–43 kJ mol⁻¹ in mineral soils [49].

Low-quality organic C limits the energy available to the microbial community [43,50]. Humic substances, complex organic molecules and recalcitrant SOM as shown by higher activation energy requirements in lower soil layers resist microbial attack and may combine with minerals to reduce microbial degradability even more [51]. As a result, higher temperatures showed disproportionate impacts on the depolymerization of high-molecular weight constituents of SOM [40]. More decomposed soil organic matter in the deepest layer is shown by the lower C:N ratios compared upper layers (Figure 1). In upper layers, cranberry plant residues show high C:N ratio of 66.7 ± 5.7 [4], indicating a decreasing gradient of C:N ratios from litter in upper soil layers and to more decomposed materials in the lower layer of cranberry soils [7].

The *Q*₁₀ values were higher (2.79 ± 0.10) in the 20–30 cm than upper (2.18 ± 0.07) layers in the range of 283–303 K in the present study. In comparison, the *Q*₁₀ values varied between 1.2 and 2.8 within temperature range of 278–308 K in the 0–29 cm layer of cropland, grassland, deciduous forest, and coniferous forest ecosystems [52]. The *Q*₁₀ values of Massachusetts forest soils in the 278–303 K range were 2.43–5.00 for hemlock, 2.62–3.77 for young birch, and 2.59–5.23 for mature birch [53]. Indeed, compared to commonly used values of 1.5–2.0, the *Q*₁₀ values may vary widely from 1 to 12 depending on land use, C:N ratio and degradability of SOM, soil class, moisture content, texture, and acidity [54]. Mycorrhizae may impact *Q*₁₀ values of carbon sources. Ericoid mycorrhizal (ErM) foliar litters, fine roots, fungal biomass and the necromass generally decomposes slower than those of arbuscular and ecto-mycorrhizal fungi, which could contribute to organic matter accumulation in sites where ErM plants occur [55]. This aspect could be further examined in cranberry agroecosystems.

5. Conclusions

The the decomposition rate of SOM in cranberry soils did not vary significantly with management (conventional vs. organic), but varied with soil layer, incubation time and temperature. The rate of CO₂ emissions decreased with elapsed time. Activation energy was 50–59 kJ mol⁻¹ in upper layers (0–20 cm) compared to 71 kJ mol⁻¹ in the 20–30 cm layer required to decompose high-molecular-weight materials. The *Q*₁₀ values were 2.9–3.1 in the deepest layer compared to 1.9–2.3 for the *Q*₁₀ values in upper layers. Temperature sensitivity of C decomposition rate in layered cranberry soils thus impacted differentially the C storage capacity of cranberry agroecosystems. Activation energy and *Q*₁₀ increased deeper in the soil, indicating higher temperature sensitivity of the most recalcitrant sources of SOM. Despite their smaller contribution to total C storage compared to upper layers of cranberry soils, the 20–30 cm soil layer would contribute increasingly to CO₂ emissions in the context of global warming.

Future research could quantify net C accumulation in cranberry soils through litter burial by sanding since the establishment of cranberry beds and the management practices required to promote C storage as ecosystem service. This will require developing a methodology for site sampling and monitoring covering several aspects of the cranberry production system to meet sustainable development goals, addressing the destruction of native ecosystems as well as the carbon already accumulated in dikes and the subsoil. Or-

ganic layers alternating with sand layers in cranberry beds and showing disproportionate contributions to CO₂ emissions could be used as sensitive markers of the impact of global warming on soil C storage capacity over decades.

Author Contributions: Conceived and designed the experiment: W.D.-Y. and N.Z.; performed the experiment: W.D.-Y.; analyzed the data: W.D.-Y. and S.-É.P.; wrote the first draft of the manuscript: W.D.-Y., S.-É.P. and L.E.P.; all authors provided critical feedback on the manuscript. All authors have read and agreed to the published version of the manuscript.

Funding: This collaborative research project was funded by Les Atocas de l'Érable Inc., Les Atocas Blandford Inc., La Cannebergière Inc., the Natural Sciences and Engineering Research Council of Canada (RDCPJ-469358-14) and Agriculture Agri-food Canada (AAFC-1555).

Institutional Review Board Statement: Not applicable.

Informed Consent Statement: Not applicable.

Data Availability Statement: Not applicable.

Conflicts of Interest: The authors declare that they have no known competing financial interests or personal relationships that could have appeared to influence the work reported in this paper.

References

1. Post, W.M.; Peng, T.-H.; Emanuel, W.R.; King, A.W.; Dale, V.H.; De Angelis, D.L. The global carbon cycle. *Am. Scient.* **1990**, *78*, 310–326.
2. Lal, R. Soil carbon stocks under present and future climate with specific reference to European ecoregions. *Nutr. Cycl. Agroecosyst.* **2008**, *81*, 113–127. [[CrossRef](#)]
3. Lal, R. Soil carbon sequestration impacts on global climate change and food security. *Science* **2004**, *304*, 1623–1628. [[CrossRef](#)] [[PubMed](#)]
4. Dossou-Yovo, W.; Parent, S.-É.; Ziadi, N.; Parent, É.; Parent, L.E. Tea Bag Index to Assess Carbon Decomposition Rate in Cranberry Agroecosystems. *Soil Syst.* **2021**, *5*, 44. [[CrossRef](#)]
5. Angers, D.A.; Chenu, C. Dynamics of soil aggregation and C sequestration. In *Soil Processes and the Carbon Cycle*; Lal, R., Kimble, J.M., Follett, R.F., Stewart, B.A., Eds.; CRC Press: Boca Raton, FL, USA, 1997; pp. 199–206.
6. Hassink, J.; Whitmore, A.P.; Kuba, J. Size and density fractionation of soil organic matter and the physical capacity of soils to protect organic matter. *Eur. J. Agron.* **1997**, *7*, 189–199. [[CrossRef](#)]
7. Kennedy, C.D.; Wilderott, S.; Payne, M.; Buda, A.R.; Kleinman, P.J.A.; Bryant, R.B. A geospatial model to quantify mean thickness of peat in cranberry bogs. *Geoderma* **2018**, *319*, 122–131. [[CrossRef](#)]
8. Stackpoole, S.M.; Kosola, K.R.; Workmaster, B.A.A.; Guldan, N.M.; Browne, B.A.; Jackson, R.D. Looking beyond fertilizer: Assessing the contribution of nitrogen from hydrologic inputs and organic matter to plant growth in the cranberry agroecosystem. *Nutr. Cycl. Agroecosyst.* **2011**, *91*, 41–54. [[CrossRef](#)]
9. Sandler, H.; DeMoranville, C. *Cranberry Production: A Guide for Massachusetts. Summary Edition*; University of Massachusetts Cranberry Station: Amherst, MA, USA, 2008; pp. 1–198.
10. Kosola, K.R.; Workmaster, B.A.A. Mycorrhizal colonization of cranberry: Effects of cultivar, soil type, and leaf litter composition. *J. Am. Soc. Hortic. Sci.* **2007**, *132*, 134–141. [[CrossRef](#)]
11. Eilers, K.G.; Debenport, S.; Anderson, S.; Fierer, N. Digging deeper to find unique microbial communities: The strong effect of depth on the structure of bacterial and archaeal communities in soil. *Soil Biol. Biochem.* **2012**, *50*, 58–65. [[CrossRef](#)]
12. Fierer, N.; Schimel, J.P.; Holden, P.A. Variations in microbial community composition through two soil depth profiles. *Soil Biol. Biochem.* **2003**, *35*, 167–176. [[CrossRef](#)]
13. Kramer, C.; Gleixner, G. Soil organic matter in soil depth profiles: Distinct carbon preferences of microbial groups during carbon transformation. *Soil Biol. Biochem.* **2008**, *40*, 425–433. [[CrossRef](#)]
14. Balesdent, J.; Basile-Doelsch, I.; Chadoeuf, J.; Cornu, S.; Derrien, D.; Fekiacova, Z.; Hatté, C. Atmosphere–soil carbon transfer as a function of soil depth. *Nature* **2018**, *559*, 599–602. [[CrossRef](#)] [[PubMed](#)]
15. Beier, C.; Rasmussen, L. Organic matter decomposition in an acidic forest soil in Denmark as measured by the cotton strip assay. *Scand. J. For. Res.* **1994**, *9*, 106–114. [[CrossRef](#)]
16. Li, J.; Yan, D.; Pendall, E.; Pei, J.; Noh, N.J.; He, J.S.; Li, B.; Nie, M.; Fang, C. Depth dependence of soil carbon temperature sensitivity across Tibetan permafrost regions. *Soil Biol. Biochem.* **2018**, *126*, 82–90. [[CrossRef](#)]
17. Davidson, E.A.; Janssens, I.A. Temperature sensitivity of soil carbon decomposition and feedbacks to climate change. *Nature* **2006**, *440*, 165–173. [[CrossRef](#)] [[PubMed](#)]
18. Bird, M.I.; Chivas, A.R.; Head, J. A latitudinal gradient in carbon turnover times in forest soils. *Nature* **1996**, *381*, 143–146. [[CrossRef](#)]

19. Von Lützow, M.; Kögel-Knabner, I. Temperature sensitivity of soil organic matter decomposition-what do we know? *Biol. Fertil. Soil* **2009**, *46*, 1–15. [[CrossRef](#)]
20. Lloyd, K.; Madramootoo, C.A.; Edwards, K.P.; Grant, A. Greenhouse gas emissions from selected horticultural production systems in a cold temperate climate. *Geoderma* **2019**, *349*, 45–55. [[CrossRef](#)]
21. Lee, C.G.; Suzuki, S.; Inubushi, K. Temperature sensitivity of anaerobic labile soil organic carbon decomposition in brackish marsh. *Soil Sci. Plant Nutr.* **2018**, *64*, 443–448. [[CrossRef](#)]
22. Sierra, C.A. Temperature sensitivity of organic matter decomposition in the Arrhenius equation: Some theoretical considerations. *Biogeochemistry* **2012**, *108*, 1–15. [[CrossRef](#)]
23. Kowalenko, C.G. Assessment of Leco CNS-2000 analyzer for simultaneously measuring total carbon, nitrogen, and sulphur in soil. *Commun. Soil Sci. Plant Anal.* **2001**, *32*, 2065–2078. [[CrossRef](#)]
24. Linn, D.M.; Doran, J.W. Effect of Water-Filled Pore Space on Carbon Dioxide and Nitrous Oxide Production in Tilled and Nontilled Soils. *Soil Sci. Soc. Am. J.* **1984**, *48*, 1267–1272. [[CrossRef](#)]
25. Verdonck, O.F.; Cappaert, I.M.; De Boodt, M.F. Physical characterization of horticultural substrates. *Acta Hortic.* **1978**, *178*, 191–200. [[CrossRef](#)]
26. Gagnon, B.; Ziadi, N.; Rochette, P.; Chantigny, M.H.; Angers, D.A.; Bertrand, N.; Smith, W.N. Soil-surface carbon dioxide emission following nitrogen fertilization in corn. *Can. J. Soil Sci.* **2016**, *96*, 219–232. [[CrossRef](#)]
27. Newton, L.S.J.; Lopes, A.; Spokas, K.; Archer, D.W.; Reicosky, D. First-order decay models to describe soil C-CO₂ loss after rotary tillage. *Sci. Agric.* **2009**, *66*, 650–657.
28. Verzani, J. *Using R for Introductory Statistics*; CRC Press: Boca Raton, FL, USA, 2018.
29. Dalgaard, P. Multiple Regression. In *Introductory Statistics with R*; Springer Science + Business Media, LLC.: Berlin/Heidelberg, Germany, 2008; pp. 185–194.
30. Cai, A.; Feng, W.; Zhang, W.; Xu, M. Climate, soil texture, and soil types affect the contributions of fine-fraction-stabilized carbon to total soil organic carbon in different land uses across China. *J. Environ. Manag.* **2016**, *172*, 2–9. [[CrossRef](#)]
31. Fissore, C.; Jurgensen, M.F.; Pickens, J.; Miller, C.; Page-Dumroese, D.; Giardina, C.P. Role of soil texture, clay mineralogy, location, and temperature in coarse wood decomposition-A mesocosm experiment. *Ecosphere* **2016**, *7*, e01605. [[CrossRef](#)]
32. McInerney, M.; Bolger, T. Temperature, wetting cycles and soil texture effects on carbon and nitrogen dynamics in stabilized earthworm casts. *Soil Biol. Biochem.* **2000**, *32*, 335–349. [[CrossRef](#)]
33. Sugihara, S.; Funakawa, S.; Kilasara, M.; Kosaki, T. Effects of land management on CO₂ flux and soil C stock in two Tanzanian croplands with contrasting soil texture. *Soil Biol. Biochem.* **2012**, *46*, 1–9. [[CrossRef](#)]
34. Ngao, J.; Epron, D.; Delpierre, N.; Bréda, N.; Granier, A.; Longdoz, B. Spatial variability of soil CO₂ efflux linked to soil parameters and ecosystem characteristics in a temperate beech forest. *Agric. For. Meteorol.* **2012**, *154–155*, 136. [[CrossRef](#)]
35. De Graaff, M.A.; Jastrow, J.D.; Gillette, S.; Johns, A.; Wullschlegel, S.D. Differential priming of soil carbon driven by soil depth and root impacts on carbon availability. *Soil Biol. Biochem.* **2014**, *69*, 147–156. [[CrossRef](#)]
36. Fontaine, S.; Barot, S.; Barré, P.; Bdioui, N.; Mary, B.; Rumpel, C. Stability of organic carbon in deep soil layers controlled by fresh carbon supply. *Nature* **2007**, *450*, 277–280. [[CrossRef](#)] [[PubMed](#)]
37. Hobbey, E.U.; Wilson, B. The depth distribution of organic carbon in the soils of eastern Australia. *Ecosphere* **2016**, *7*, e01214. [[CrossRef](#)]
38. Bonan, G.B.; Hartman, M.D.; Parton, W.J.; Wieder, W.R. Evaluating litter decomposition in earth system models with long-term litterbag experiments: An example using the Community Land Model version 4 (CLM4). *Glob. Change Biol.* **2013**, *19*, 957–974. [[CrossRef](#)]
39. Cornwell, W.K.; Cornelissen, H.C.; Dorrepaal, E.; Eviner, V.T.; Godoy, O.; Hobbey, S.E.; Hoorens, B.; Van Bodegom, P. Plant species traits are the predominant control on litter decomposition rates within biomes worldwide. *Ecol. Lett.* **2008**, *11*, 1065–1071. [[CrossRef](#)]
40. Duboc, O.; Zehetner, F.; Djukic, I.; Tatzber, M.; Berger, T.W.; Gerzabek, M.H. Decomposition of European beech and black pine foliar litter along an Alpine elevation gradient: Mass loss and molecular characteristics. *Geoderma* **2012**, *189*, 522–531. [[CrossRef](#)]
41. Jobbágy, E.G.; Jackson, R.B. The vertical distribution of soil organic carbon and its relation to climate and vegetation. *Ecol. Appl.* **2000**, *10*, 423–436. [[CrossRef](#)]
42. Schrumpf, M.; Kaiser, K.; Guggenberger, G.; Persson, T.; Kögel-Knabner, I.; Schulze, E.-D. Storage and stability of organic carbon in soils as related to depth, occlusion within aggregates, and attachment to minerals. *Biogeosciences* **2013**, *10*, 1675–1691. [[CrossRef](#)]
43. Bosatta, E.; Ågren, G.I. Soil organic matter quality interpreted thermodynamically. *Soil Biol. Biochem.* **1999**, *31*, 1889–1891. [[CrossRef](#)]
44. Hicks Pries, C.E.; Sulman, B.N.; West, C.; O'Neill, C.; Poppleton, E.; Porras, R.C.; Castanha, C.; Zhu, B.; Wiedemeier, D.B.; Torn, M.S. Root litter decomposition slows with soil depth. *Soil Biol. Biochem.* **2018**, *125*, 103–114. [[CrossRef](#)]
45. Kuzyakov, Y. Priming effects: Interactions between living and dead organic matter. *Soil Biol. Biochem.* **2010**, *42*, 1363–1371. [[CrossRef](#)]
46. St-Luce, M.; Ziadi, N.; Chantigny, M.H.; Braun, J. Long-term effects of tillage and nitrogen fertilization on soil C and N fractions in a corn–soybean rotation. *Can. J. Soil Sci.* **2022**, *102*, 277–292. [[CrossRef](#)]
47. Andlar, M.; Rezić, T.; Marđetko, N.; Kracher, D.; Ludwig, R.; Šantek, B. Lignocellulose degradation: An overview of fungi and fungal enzymes involved in lignocellulose degradation. *Eng. Life Sci.* **2018**, *18*, 768–778. [[CrossRef](#)] [[PubMed](#)]

48. Steinweg, J.M.; Jagadamma, S.; Frerichs, J.; Mayes, M.A. Activation energy of extracellular enzymes in soils from different biomes. *PLoS ONE* **2013**, *8*, e59943. [[CrossRef](#)] [[PubMed](#)]
49. Parent, L.E.; Mackenzie, A.F. Rate of Pyrophosphate Hydrolysis in Organic Soils. *Can. J. Soil Sci.* **1985**, *65*, 497–506. [[CrossRef](#)]
50. Fierer, N.; Craine, J.M.; McLauchlan, K.K.; Schimel, J.P. Litter quality and the temperature sensitivity of decomposition. *Ecology* **2005**, *86*, 320–326. [[CrossRef](#)]
51. Gerke, J. Concepts and misconceptions of humic substances as the stable part of soil organic matter: A review. *Agronomy* **2018**, *8*, 76. [[CrossRef](#)]
52. Meyer, N.; Welp, G.; Amelung, W. The temperature sensitivity (Q_{10}) of soil respiration: Controlling factors and spatial prediction at regional scale based on environmental soil classes. *Glob. Biogeochem. Cycl.* **2018**, *32*, 306–323. [[CrossRef](#)]
53. Ignace, D.D. Determinants of temperature sensitivity of soil respiration with the decline of a foundation species. *PLoS ONE* **2019**, *14*, e0223566. [[CrossRef](#)]
54. Meyer, N.; Meyer, H.; Welp, G.; Amelung, W. Soil respiration and its temperature sensitivity (Q_{10}): Rapid acquisition using mid-infrared spectroscopy. *Geoderma* **2018**, *323*, 31–40. [[CrossRef](#)]
55. Ward, E.B.; Duguid, M.C.; Kuebbing, S.E.; Lendemer, J.C.; Warren II, R.J.; Bradford, M.A. Ericoid mycorrhizal shrubs alter the relationship between tree mycorrhizal dominance and soil carbon and nitrogen. *J. Ecol.* **2021**, *109*, 3524–3540. [[CrossRef](#)]

Disclaimer/Publisher’s Note: The statements, opinions and data contained in all publications are solely those of the individual author(s) and contributor(s) and not of MDPI and/or the editor(s). MDPI and/or the editor(s) disclaim responsibility for any injury to people or property resulting from any ideas, methods, instructions or products referred to in the content.